Journal of Power Sources 195 (2010) 2628–2632

Contents lists available at ScienceDirect

Journal of Power Sources

journal homepage: www.elsevier.com/locate/jpowsour

Functionally-graded composite cathodes for durable and high performance solid oxide fuel cells

Hwa Seob Song[a], Seungho Lee[a], Daehee Lee[a], Hongyeun Kim[a], Sang Hoon Hyun[a], Joosun Kim[b], Jooho Moon[a,*]

[a] Department of Materials Science and Engineering, Yonsei University, Seoul 120-749, Republic of Korea
[b] Center for Energy Materials Research, Korea Institute of Science and Technology, Seoul 136-791, Republic of Korea

ARTICLE INFO

Article history:
Received 1 July 2009
Received in revised form
25 September 2009
Accepted 6 November 2009
Available online 24 November 2009

Keywords:
Solid oxide fuel cell composite cathode
Functionally-graded layer
Durability

ABSTRACT

A double-layer dual-composite cathode is fabricated and has an ideal cathode microstructure with large electrochemical active sites and enhanced the durability in solid oxide fuel cells (SOFCs). The insertion of a yttria-stabilized zirconia (YSZ)-rich functional layer between the electrolyte and the electrode allows for a graded transition of the YSZ phase, which enhances ionic percolation and minimizes the thermal expansion coefficient mismatch. Electrochemical measurements reveal that the double-layer composite cathode exhibits improved cathodic performance and long-term stability compared with a single-layer composite cathode. A cell with a well-controlled cathode maintains nearly constant interfacial polarization resistance during an 80 h accelerated lifetime test.

1. Introduction

Solid oxide fuel cells (SOFCs) are power-generating systems that can potentially replace conventional stationary power-plants, internal-combustion engines in automobiles, and battery-based portable power units. The most critical obstacles to the successful commercialization of SOFCs are deficiencies in reliability and durability. The reliability issues stem from the high operating temperatures that degrade cell components, even though SOFCs permit heat and power co-generation at improved efficiency. Therefore, the goal of recent research has been to develop cell components that are stable at high operating temperatures, and that would improve the reliability and cost competitiveness of SOFC systems [1–6].

In previous reports, engineered LSM-YSZ dual-composite particles were introduced, in which both the LSM and YSZ phases were placed (conjugated) on a YSZ core to produce a high performance durable cathode [7,8]. The use of this dual-composite approach allows for the development of an ideal cathode microstructure with improved phase contiguity and interfacial coherence. In particular, the volume fraction of the conjugated YSZ phase with respect to the YSZ core plays a critical role in maintaining electrode durability while allowing for good cell performance. The amount of the conjugated YSZ phase needs to be optimized. Above the optimum composition, the cathodes are durable but show high polarization resistance, while below the optimal value, they have low polarization resistance and undergo degradation during high-temperature operation.

In the present study, functionally-graded cathode structures are introduced to improve electrode performance and durability [9,10]. A functionally-graded cathode is composed of a functional layer and an electrochemical active layer with different compositions, as shown in Fig. 1. A thin functional layer with a conjugated YSZ phase-rich dual-composite (conjugated LSM: YSZ core: conjugated YSZ = 37:42:21 by volume) is placed in contact with the electrolyte to enhance the connectivity and ionic percolation between the electrolyte and the cathode. A thick electrochemical active layer comprised of a conjugated LSM phase-rich dual-composite (conjugated LSM: YSZ core: conjugated YSZ = 47:42:11 by volume) is introduced on top of the functional layer to provide sufficient reaction sites. This double-layer cathode has a graded interface across which the composition gradually changes from one layer to another and is specifically tuned for long-term durability and high cathodic performance.

2. Experimental

LSM ($La_{0.85}Sr_{0.15}MnO_3$)-YSZ composite powder was prepared via the polymerizable complex method [11]. To synthesize LSM-YSZ dual-composite (denoted *LYDC*) particles, YSZ core particles (Tosoh TZ8Y, surface area = 12.74 $m^2\,g^{-1}$, mean particle

* Corresponding author. Tel.: +82 2 2123 2855; fax: +82 2 365 5882.
E-mail address: jmoon@yonsei.ac.kr (J. Moon).

0378-7753/$ – see front matter © 2009 Elsevier B.V. All rights reserved.
doi:10.1016/j.jpowsour.2009.11.067

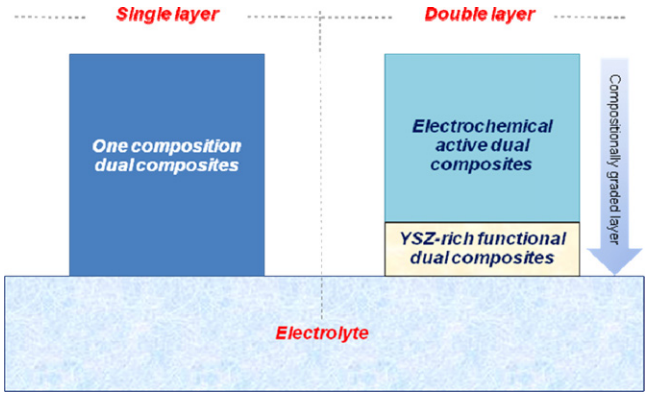

Fig. 1. Cross-sectional illustrations of single- and double-layer composite cathodes.

size = 78 nm) were suspended in polymeric resin obtained by esterification between metal ions (La, Sr, Mn, Y, and Zr), an organic complex, and ethylene glycol. Upon calcination at 1000 °C for 2 h, the polymeric resin was transformed into LSM and YSZ conjugated on the YSZ core. The resulting LYDC consisted of approximately 30–50 nm-sized LSM and YSZ nanoparticles attached to the core particles. For the functional layer, composite particles with a composition of conjugated LSM: YSZ core: conjugated YSZ = 37:42:21 by volume (denoted *LYDC 37-42-21*) were synthesized.

The cathode layers were deposited on a YSZ disc (sintered at 1400 °C, thickness = 0.5 mm, diameter = 20 mm) by screen printing and sintered at 1100 °C for 4 h. The area of the applied cathode was 1.4 cm^2, and its thickness was about 25 μm. Two types of electrode structures were tested as shown in Fig. 1: (i) a single-layer cathode with a composition of either *LYDC 47-42-11* or *47-23-30* and (ii) a double-layer cathode with *LYDC 37-42-21* as a functional layer and *LYDC 47-42-11* as an active layer. An NiO-YSZ anode-supported cell with the composite cathode was also fabricated. The NiO-YSZ anode supports were prepared by pressing the polymeric resin-derived nanocomposite powders [12]. A YSZ electrolyte with a thickness of 6–7 μm was placed on the anode support via the dip-coating method. After sintering at 1400 °C for 4 h, one side of the support was polished to remove the YSZ electrolyte and to adjust the anode support thickness to ~1.0 mm. After the deposition of the cathode, platinum mesh and nickel felt were used as current collectors on the cathode and anode layers, respectively.

The cross-sectional microstructures of the composite cathodes were investigated by means of field emission scanning electron microscopy (FE-SEM, JSM 6700F, JEOL). An electron probe micro-analyzer (EPMA, EPMA1600, Shimadzu) was also used to analyze the compositional distribution. The porosity and the pore sizes of the composite electrodes were determined by mercury porosimetry (Autopore IV 9500, Micromeritics Instrument Corp.). Electrochemical impedance measurements were performed on symmetrical cells using ac impedance spectroscopy (Solartron SI 1260/1287) [13–16]. A pyramid-type cyclic current load was employed for the accelerated lifetime test (ALT). Each load consisted of a cyclic current load applied at 0.14–0.71 A cm^{-2}, and each cycle lasted 30 min. After applying this load, impedance spectra were gathered. Full-cell performance was also measured using humidified hydrogen as fuel and air as an oxidant at ambient pressure and a temperature of 800 °C.

3. Results and discussion

A cross-sectional view of the double-layer composite cathode (*LYDC 37-42-21/47-42-11*) is shown in Fig. 2a. The thin functional layer is ~5 μm-thick and consistes of 37 vol.% LSM/63 vol.% YSZ dual-composite particles. The active layer is ~20 μm-thick

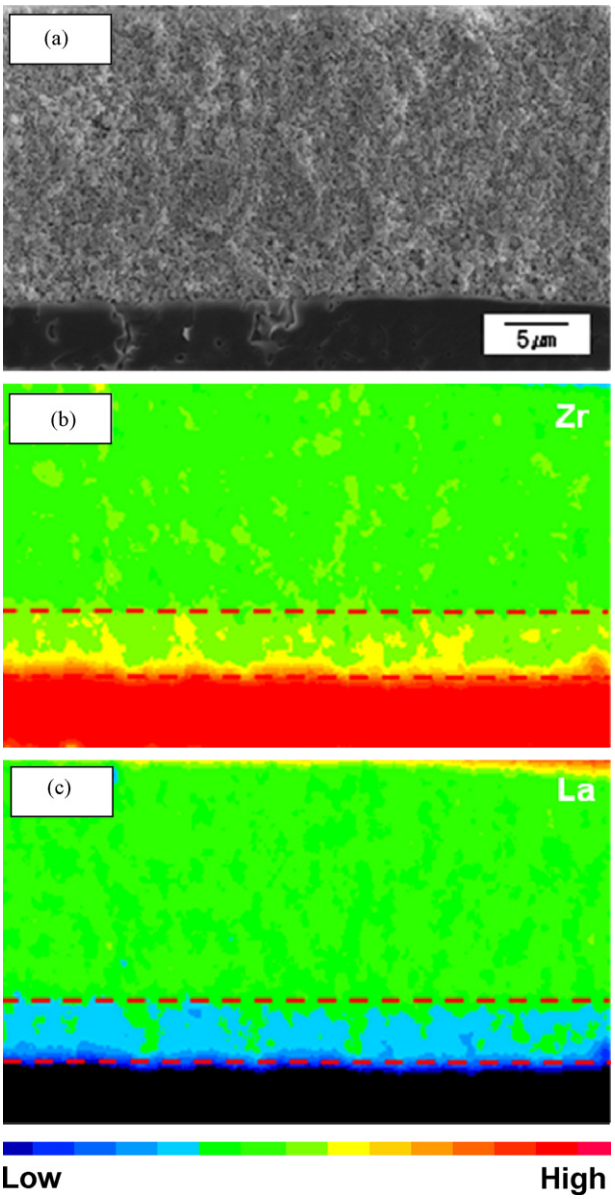

Fig. 2. (a) Cross-sectional fractured surface of functionally-graded cathode fabricated on a YSZ pellet, (b) EPMA mapping showing Zr distribution on cross-sectional surface, and (c) EPMA mapping of La distribution.

and is composed of 47 vol.% LSM/53 vol.% YSZ. Observation of the microstructure by SEM is unable to distinguish between the functional layer and the active layer since both have similar porosities and microstructural features. By contrast, EPMA analysis revealed gradual compositional changes in the cross-sectional micrograph. As shown in Fig. 2b, the Zr content decreases from the electrolyte to the LSM-YSZ surface, while the La distribution exhibites the opposite trend (Fig. 2c). The cathode layers are structured as shown in Fig. 2a. It is thought that the use of a YSZ-rich functional layer will provide better ionic conduction and high stability, whereas the LSM-rich top layer will offer high reaction activity for oxygen reduction and high electron conductivity. Mercury porosimetry results show that all of the composite cathodes have narrow pore size distributions with a mean pore size of 135–156 nm. The porosities of the composites are between 44% and 45%.

The total interfacial resistance for the dual-composite cathodes with different compositions is presented in Fig. 3 (a). The total inter-

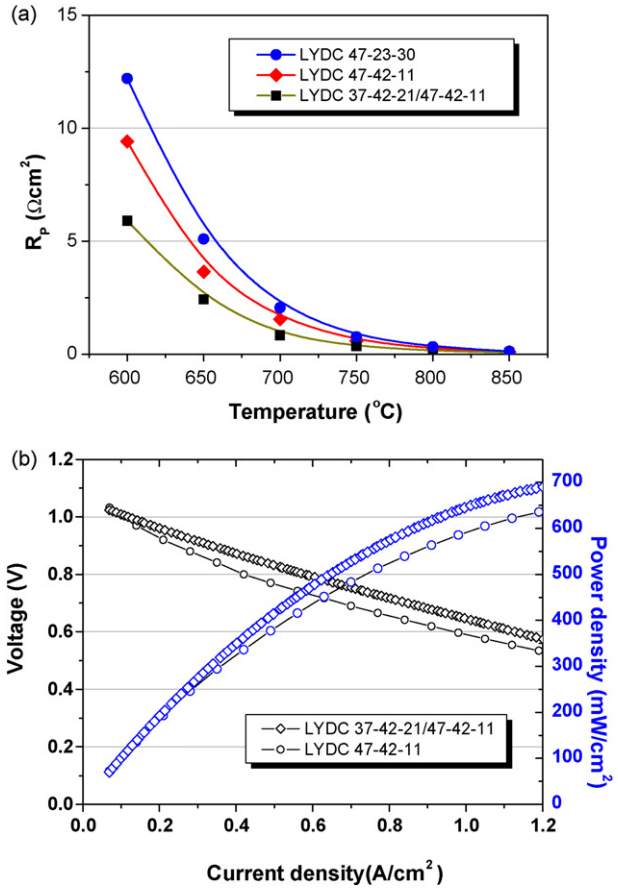

Fig. 3. (a) Total interfacial polarization (R_p) resistance of composite cathode where $R_P = R_A + R_B$. Impedance spectra were obtained in air at 600–850 °C using a symmetrical cell as a function of operating temperature. (b) Electrochemical performance of anode-supported fuel cells based on *LYDC 37-42-21/47-42-11* and *47-42-11* cathodes at 800 °C.

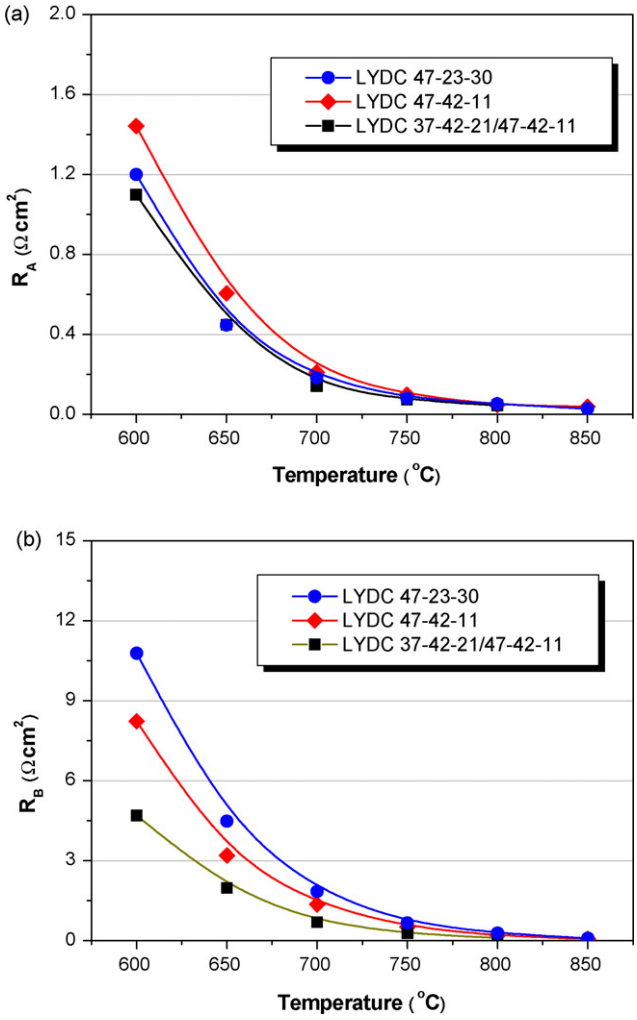

Fig. 4. (a) Polarization resistance of *Process A* (R_A) and (b) *Process B* (R_B). Impedance spectra obtained in air at 600–850 °C using a symmetrical cell as a function of operating temperature.

facial polarization resistance of the double-layer cathode with *LYDC 37-42-21/47-42-11* is much lower than those of the single-layer cathodes composed of either *LYDC 47-42-11* or *47-23-30*. For example, the resistance of the double-layer cathode is only 0.138 Ω cm^2 at 800 °C compared with 0.236 Ω cm^2 for the single-layer *LYDC 47-42-11*. To the best of our knowledge, this interfacial resistance is one of the lowest values among those reported for LSM-YSZ-based composite cathodes. The insertion of a YSZ-rich functional layer (37 vol.% LSM/63 vol.% YSZ) resulted in significant improvement in the cathodic performance compared with the single-layer cathodes with an LSM-rich composition (47 vol.% LSM/53 vol.% YSZ). The power densities of the cells with different cathodes at 800 °C are shown in Fig. 3b. The open-circuit voltage is 1.05 V, which indicates no gas crossover and negligible electronic conductivity in the electrolyte. The maximum power density of a cell with a double-layer cathode is 720 mW cm^{-2}, whereas the maximum power density of a cell with a single-layer cathode (*LYDC 47-42-11*) is 650 mW cm^{-2}.

The measured total interfacial polarization resistance (R_P) can be resolved into elementary reaction steps to better understand the electrode process. Previously, it was demonstrated that the impedance spectra of LSM-YSZ cathodes are well fitted by a model with two major arcs, denoted *Process A* (high frequency) and *Process B* (low frequency). The resistance for *Process A* (R_A) is related to the YSZ phase interconnectivity that reflects the transport and transfer of oxide ions at the interfaces and the YSZ phase of the composite, whereas R_B for *Process B* reflects the electrochemical activity of oxygen reduction at a triple-phase boundary (TPB) [17].

Analysis of the resolved resistances (R_A and R_B) allows for an understanding of the microstructural features associated with the functionally-graded cathodes. As shown in Fig. 4a, R_A (which reflects the YSZ phase interconnectivity) of the double-layer cathode is even lower than that of the *LYDC 47-23-30* single-layer cathode, which is considered to have a stable and firm YSZ skeleton structure due to the presence of more of the conjugated YSZ phase. The double-layer cathode also displays a smaller R_B, which is related to the TPB site density, as compared with the *LYDC 47-42-11* single-layer composite cathode, in which the reduced amount of the YSZ-conjugated phase with respect to LSM is believed to enhance the LSM/YSZ contact points (Fig. 4b). This observation implies the simultaneous enhancement of ionic percolation and enlargement of the TPB site density, which is generally difficult to achieve without a compromise. The double-layer composite cathode with graded compositions benefits from the synergetic effect of the YSZ-rich functional layer (*LYDC 37-42-21*) inserted between the electrolyte and the electrode. Holtappels and Bagger [18] demonstrated that the ionic in-plane conductivity of a cathode was improved by grading with a better conducting phase where the individual optimized structures of the graded electrode allow maximum diffusion of air and oxygen ions at the triple-phase boundaries [18]. Thus, ionic conductivity and percolation play important roles in determining the cathodic performance. A YSZ-rich functional layer can extend the ionically-conductive area into the electrode

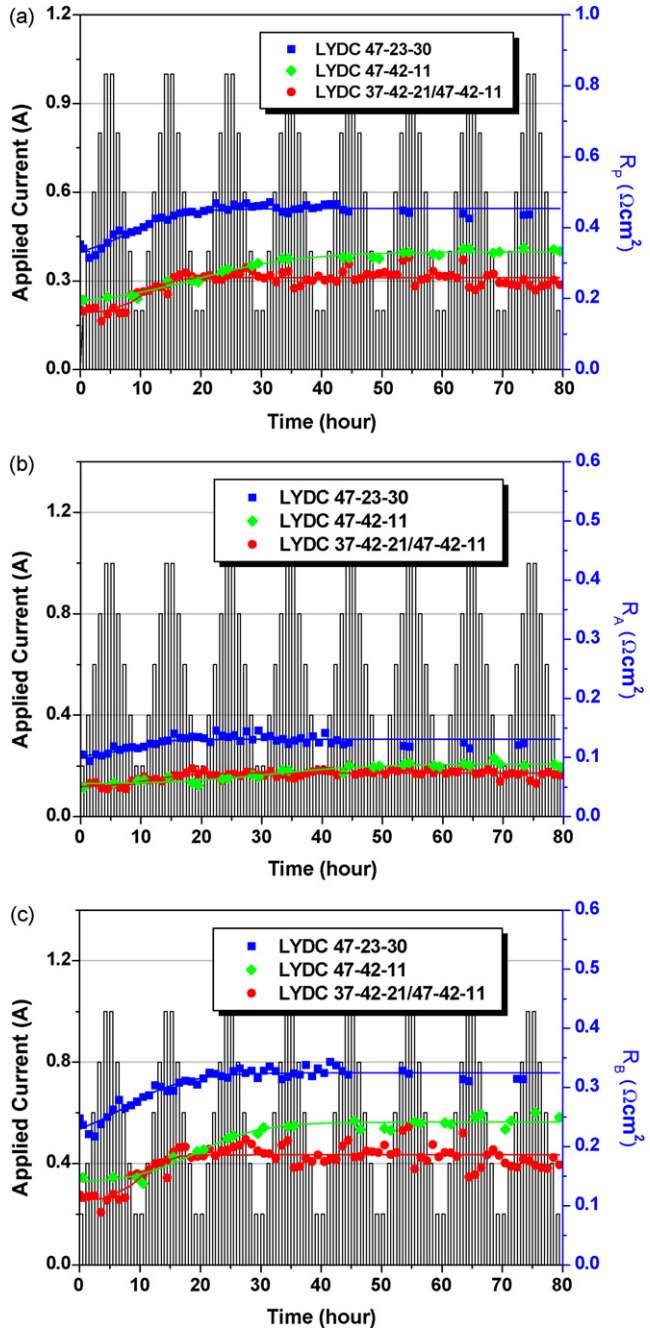

Fig. 5. Variations of area specific resistance for three different composite cathodes in a symmetric cell configuration during accelerated lifetime tests (ALT) at 800 °C: (a) total interfacial polarization resistance (R_P) and ALT profile, (b) polarization resistance for *Process A* (R_A), and (c) polarization resistance for *Process B* (R_B).

region. This brings about improved oxygen reduction on the electrode, manifested by reduced R_A and R_B values. The *LYDC 37-42-21* single-layer composite cathode has a greater polarization resistance (results not shown here) then double-layer cathode. This indicated that the YSZ-rich functional layer should be limited to a thin region (~5 μm in the present study).

The YSZ-rich functional layer is also expected to provide mechanical and electrochemical long-term stability. For assessing the long-term stability of the composite cathodes, accelerated lifetime tests (ALTs) [19] were performed. The resolved interfacial polarization resistance variations during the ALTs at 800 °C for half-cells with three different composite cathodes are shown in Fig. 5. The total interfacial polarization resistance (R_P) of the cells with *LYDC 47-23-30*, *47-42-11*, and *37-42-21/47-42-11* at the initial stage is 0.353, 0.197, and 0.168 Ω cm^2, respectively (Fig. 5a). After an 80 h current load, the resistances of *LYDC 47-23-30, 47-42-11,* and *37-42-21/47-42-11* increase by 24.1%, 69.0%, and 42.9%, respectively. The near invariance of the polarization resistance for the single-layer *LYDC 47-23-30* cathode can be attributed to the presence of more of the YSZ-conjugated phase. It is characterized by a high R_p value, which is indicative of lower cathodic performance. As shown in Fig. 5b, the R_A increases from 0.049 to 0.084 Ω cm^2 for the *LYDC 47-42-11* single-layer cathode, while it remains nearly constant (from 0.05 to 0.07 Ω cm^2) for the double-layer cathode. The R_B of the *LYDC 47-42-11* single-layer cathode increases from 0.148 to 0.25 Ω cm^2, whereas the R_B of the double-layer cathode changed slightly from 0.12 to 0.17 Ω cm^2, as shown in Fig. 5c. The single-layer cathode with the LSM-rich composition (*LYDC 47-42-11*) undergoes a microstructural change during the ALT due to LSM coarsening [7]. The double-layer cathode with well-engineered graded compositions exhibits a remarkably low polarization resistance and long-term durability. The introduction of a thin YSZ-rich functional layer enhances the long-term thermochemical and electrochemical stabilities as a result of a diminished thermal expansion coefficient mismatch and an improved interfacial coherence. The slight increase in the polarization resistance originates from minor degradation of the electrochemically active layer.

4. Conclusions

A functionally-graded nanostructured composite cathode is fabricated using engineered dual-composite particles for improvements in electrode performance and durability. The fabricated cathode has a compositionally-graded interface in which the YSZ content gradually changes from the electrolyte side to the top cathode side and is specifically tuned for long-term stability and high cathodic performance. The use of the nanostructured double-layer with dual-composite particles allows the development of an ideal cathode microstructure with improved phase contiguity, thermal expansion coefficient compatibility, and electrochemical activity. The double-layer composite cathode with a well-engineered composition exhibits low interfacial polarization resistances and high power densities as well as long-term reliability compared with those of the composite cathodes with a single composition.

Acknowledgements

This work is the outcome of the fostering project of the Specialized Graduate School of Hydrogen & Fuel Cells and was financially supported by the Ministry of Commerce, Ministry of Knowledge Economy (MKE), Industry and Energy (MOCIE), and Seoul R&BD Program (CS070157). The study was also partially supported by the Korea Science and Engineering Foundation (KOSEF) through the National Research Lab Program funded by the Ministry of Education, Science, and Technology (No. R0A-2005-000-10011-0).

References

[1] S. Singhal, K. Kendall, High-Temperature Solid Oxide Fuel Cells: Fundamentals Design and Applications, Elsevier, Oxford, 2003.
[2] E. Ivers-Tiffée, A. Weber, D. Herbstritt, J. Eur. Ceram. Soc. 21 (2001) 1805–1811.
[3] M. Mogensen, S. Skaarup, Solid State Ionics 86/88 (1996) 1151–1160.
[4] T.Z. Sholklapper, V. Radmilovic, C.P. Jacobson, S.J. Visco, L.C. De Jonghe, Electrochem. Solid-State Lett. 10 (4) (2007) B74–B76.
[5] E. Ivers-Tiffee, A. Weber, K. Schmid, V. Kerbs, Solid State Ionics 174 (2004) 223–232.
[6] M. Kuznecov, P. Otschik, P. Obenaus, K. Eichler, W. Schaffrath, Solid State Ionics 157 (2003) 371–378.
[7] H.S. Song, S.H. Hyun, J. Kim, H.-W. Lee, J. Moon, J. Mater. Chem. 18 (2008) 1087–1092.
[8] H.S. Song, S. Lee, S.H. Hyun, J. Kim, J. Moon, J. Power Sources 187 (2009) 25–31.

[9] S. Zha, Y. Zhang, M. Liu, Solid State Ionics 176 (2005) 25–31.
[10] X. Xu, C. Xia, G. Xiao, D. Peng, Solid State Ionics 176 (2005) 1513–1520.
[11] M. Kakihana, M. Arima, M. Yoshimura, N. Ikeda, Y. Sugitani, J. Alloys Compd. 283 (1999) 102–105.
[12] S.-D. Kim, H. Moon, S.-H. Hyun, J. Moon, J. Kim, H.-W. Lee, J. Power Sources 163 (2006) 392–397.
[13] M.J. Jorgensen, M. Mogensen, J. Electrochem. Soc. 148 (2001) A433–A442.
[14] E.M. Skou, T. Jacobsen, Appl. Phys. A 49 (1989) 117–121.
[15] J. Fleig, P. Pham, P. Sztulzaft, J. Maier, Solid State Ionics 113–115 (1998) 739–747.
[16] M.J.L. Østergard, M. Mogensen, Electrochim. Acta 38 (14) (1993) 2015–2020.
[17] H.S. Song, W.H. Kim, S.H. Hyun, J. Moon, J. Kim, H.-W. Lee, J. Power Sources 167 (2007) 258–264.
[18] P. Holtappels, C. Bagger, J. Eur. Ceram. Soc. 22 (2002) 41–48.
[19] W. Nelson, Accelerated Life Testing: Statistical Models Test Plans and Data Analysis, John Wiley & Sons, New York, 1990.